International Journal of Non-Linear Mechanics 83 (2016) 1–8

Contents lists available at ScienceDirect

International Journal of Non-Linear Mechanics

journal homepage: www.elsevier.com/locate/nlm

Probabilistic solution of non-linear random ship roll motion by path integration

H.T. Zhu *, L.L. Duan

Key Laboratory of Coast Civil Structure Safety of Ministry of Education, Tianjin University, Tianjin 300072, People's Republic of China

ARTICLE INFO

Article history:
Received 6 July 2015
Received in revised form
8 January 2016
Accepted 30 March 2016
Available online 1 April 2016

Keywords:
Path integration
Ship roll motion
Probability density function
Numerical solution

ABSTRACT

This paper investigates the probability density function (PDF) of non-linear random ship roll motion using a previously developed path integration method. The mathematical model of ship rolling motion consists of a linear-plus-cubic damping and a non-linear restoring moment in the form of odd-order polynomials up to fifth-order terms. In the path integration method, the interpolation scheme is based on the Gauss–Legendre quadrature integration rule and the short-time transition probability density function is formulated by short-time Gaussian approximation. The present work extends the path integration method to the case of non-linear random ship roll motion. Different values of non-linearity coefficient and excitation intensity are used to examine the effectiveness of the path integration method. Numerical analysis shows that the results of the path integration method agree well with the simulation results, even in the tail region. The path integration method is effective and it is simply implemented in the examined cases. Due to the presence of non-linear damping terms and non-linear restoring moment terms, the PDFs of roll angle and angular velocity exhibit highly non-Gaussian behaviors.

1. Introduction

The reliability design of mechanical and structural systems is a crucial issue when these systems are excited by random excitations, such as wind, sea wave and earthquake ground motion. When seeking the failure probability of these systems, the response probability density function (PDF) has to accurately be obtained exactly or approximately. When a system is excited by Gaussian white noise or filtered Gaussian white noise, the response of the system can be regarded as a Markov process. The corresponding PDF evolution is governed by a parabolic partial differential equation which is called as the Fokker–Planck–Kolmogorov (FPK) equation. However, the FPK equation cannot be easily solved exactly in most cases. Only a few exact stationary solutions are available in some very special cases [1–3]. Most work has to appeal to approximate or numerical approaches. Some conventional methods include equivalent linearization method [4–6], stochastic averaging method [7], cumulant-neglect closure method [8], finite element method [9,10], finite difference method [11], Monte Carlo simulation [12] and path integration method [13,14]. In particular, the path integration method has been receiving much attention in the past decades. The path integration method is based on approximate solutions of the FPK equation in short-time steps. The basic idea is that a long-term PDF evaluation can be expressed in a series of shorter-term evolutions [15,16]. It can provide an accurate PDF even at very low probability levels. There are three important aspects to be addressed for a conventional path integration method, namely transition probability density function, interpolation scheme and discretization process in space and time.

Many efforts have been devoted to developing different transition PDFs and interpolation techniques. Wehner and Wolfer made an early systematic study to develop the path integration method into a numerical tool [13,17,18]. They used a piecewise constant interpolation scheme and their numerical results had lower values near the peaks and higher values at the tails in the probability distribution. They suggested that the numerical accuracy could be improved with an adequate interpolation scheme. Hsu and Chiu introduced another kind of numerical path integration method called as a cell mapping method [19,20]. It included the simple cell mapping and the generalized cell mapping. The basic idea was to consider the state space not as a continuum but rather as a collection of a large number of state cells with each cell being treated as a state entity. Subsequently, Sun and Hsu proposed a short-time Gaussian approximation scheme for the transition PDF in the generalized cell mapping method [21,22]. The examined oscillators included a one-dimensional system with a cubic-order displacement term, a van der Pol oscillator and a Dimentberg oscillator [2]. Similarly, Crandall et al. conducted much earlier work on numerical diffusion techniques for solving

* Corresponding author.
E-mail address: htzhu@tju.edu.cn (H.T. Zhu).

http://dx.doi.org/10.1016/j.ijnonlinmec.2016.03.010
0020-7462/

some first-passage problems in random vibration [23,24]. Their techniques were also related to the path integration method [14–16]. The common idea of the above three methods is that the evolution of probability density over time is computed successively over short-time steps. Naess and Johnsen used stochastic differential equations to formulate a Gaussian transition PDF and they applied cubic B-splines to perform an interpolation procedure [14]. Later Naess and Moe applied a splines interpolation method to the logarithm of the calculated PDF to obtain an accurate representation of the PDF [25]. They studied some conventional oscillators, e.g., Duffing oscillators and a Dimentberg oscillator [2]. Yu et al. proposed a Gauss–Legendre integration scheme to improve the computational efficiency and accuracy of the path integration method [15,16]. The Gauss–Legendre quadrature integration rule was further studied on the Ornstein–Uhlenbeck system, a Duffing oscillator and a non-linear oscillator with non-linear damping. Wang proposed a closed Newton–Cotes quadrature integration scheme [26]. The computational efficiency of the numerical integration scheme was found to be very high. Compared with the Gauss–Legendre scheme, the Newton–Cotes algorithm was easy to develop because Newton–Cotes quadrature used values of the integrand at equally spaced abscissas and the values of the quadrature coefficients were easily calculated.

Another direction on path integration methods is their application to solving different types of problems. Pirrotta and Santoro applied a path integration method to studying the probabilistic response of non-linear systems under combined normal and Poisson white noise [27]. A non-linear system under normal white noise, under Poissonian white noise and under the superposition of normal and Poisson white noise was studied, respectively. Cottone et al. employed a path integration method to study the response of ship roll motion under parametric normal white noise and additive Poisson white noise [28]. Kougioumtzoglou and Spanos developed an analytical Wiener path integral technique for non-stationary response determination of non-linear oscillators [29]. Relying on the methods of statistical linearization and of stochastic averaging, an approximate closed form solution has been determined for the non-stationary response amplitude PDF of a class of oscillators with linear stiffness and non-linear damping. A van der Pol oscillator, a Rayleigh oscillator, and a linear-plus-cubic damping oscillator have been considered to show the effectiveness of the method. Later they employed a numerical path integral approach to obtain response and first-passage PDFs for a softening Duffing oscillator under random loading [30]. First-passage PDFs were derived by assuming a special form for the conditional PDF of the system response amplitude. This assumption relied on the Markov properties of the response process and on a discrete version of the Chapman–Kolmogorov equation. Dimentberg et al. applied a path integration method to analyzing random vibrations with strongly inelastic impacts [31]. With the help of Zhuravlev–Ivanov transformation, a new system without velocity jumps was formulated, which was further handled by the path integration method. They followed the path integration procedure developed by Naess et al. [14,25]. Liu and Tang adopted a path integration method to study the random jumping of ship rolling under filtered Gaussian white noise considering the static effect of liquid on board [32]. Their solution procedure followed the path integration procedure developed by Naess and Moe [25]. Using the idea of Sun and Hsu [21,22], Köylüoglu et al. adopted a path integration method to study the PDF of a Duffing oscillator under Poisson impulses [33,34]. Their path integration method was more suitable in the case of relatively low impulse arrival rates because the transition probability matrix was calculated assuming the transition time interval to be sufficiently small so that at most one pulse was likely to occur during the interval. Di Paola and Santoro also adopted a path integration method for studying non-linear system enforced by Poisson white noise [35,36]. They developed an explicit expression of the path integration method for the case of Poisson white noise. Wang et al. followed the Gauss–Legendre integration scheme of Yu et al. [15,16] to study the strongly non-linear stochastic systems [37], the response of a moored vessel excited by slowly varying non-Gaussian wave drift forces [38] and the extreme response exceedance probabilities of a moored floating cylinder excited by slowly varying wave drift forces [39], respectively. In their study, the Duffing oscillator was adopted to model non-linear stochastic systems. The higher-order non-linear terms (e.g., a fifth-order non-linearity term) were not considered. More recently, Chai et al. followed the path integration scheme of Naess and his coworkers [14,25] to formulate a four-dimensional path integration method to study the stochastic roll response and reliability of a vessel in random beam seas [40]. The four-dimensional dynamical system consisted of a single-degree-of-freedom ship rolling motion and a second-order linear filter approximating the stationary roll excitation moment. The linear-plus-cubic restoring terms were considered. They found that the non-linear effects associated with the restoring terms and the damping terms had a significant influence on the response statistics in the large roll response region. The corresponding linear terms mainly influenced the response statistics in the low roll response region.

From the above description, although there are considerable efforts on developing the path integration method for its implementation and applications, more engineering problems are still worth investigating with the path integration method. This paper presents a path integration analysis on non-linear random ship roll motion. The mathematical model of ship roll motion consists of a linear-plus-cubic damping and a non-linear restoring moment in the form of odd-order polynomials up to fifth-order terms. As the adopted path integration method is concerned, the interpolation scheme is based on the Gauss–Legendre quadrature integration rule [15,16] and the short-time transition probability density is based on short-time Gaussian approximation [21,22]. The present work extends the path integration method to the case of non-linear random ship roll motion. Different values of non-linearity coefficient and excitation intensity are used to examine the effectiveness of the path integration method. Numerical analysis shows that the path integration solutions agree well with the results given by Monte Carlo simulation, even in the tail region of probability density. The path integration method is effective and simply implemented in the examined cases. For short-time Gaussian approximation, the Gaussian closure method is used. The cumulant expansion procedure follows the techniques presented in Refs. [41–43].

2. Path integration method

One of the mathematical models for non-linear random ship roll motion can be expressed as follows:

$$\ddot{x} + c_1\dot{x} + c_3\dot{x}^3 + k_1x + k_3x^3 + k_5x^5 = W(t) \tag{1}$$

where x, $\dot{x}$ and $\ddot{x}$ denote roll angle, angular velocity and angular acceleration, respectively. c_1 and c_3 denote the coefficients of linear and third-order damping terms, respectively. k_1, k_3 and k_5 denote the coefficients of linear, third-order and fifth-order restoring terms, respectively. $W(t)$ denotes a zero mean Gaussian white noise, which is characterized by

$$E[W(t)] = 0 \tag{2}$$

$$E[W(t)W(t+\tau)] = 2\pi K\delta(\tau) \tag{3}$$

where $2\pi K$ denotes the excitation intensity and $\delta(\bullet)$ is the Dirac delta function.

Letting $\dot{x} = v$,

$$\begin{cases} \dot{x} = v \\ \dot{v} = -c_1 v - c_3 v^3 - k_1 x - k_3 x^3 - k_5 x^5 + W(t) \end{cases} \tag{4}$$

Correspondingly, the PDF $q(x, v, t|x^{(0)}, v^{(0)}, t_0)$ of x and v is governed by the FPK equation

$$\frac{\partial q}{\partial t} = -v\frac{\partial q}{\partial x} + \frac{\partial}{\partial v}[(c_1 v + c_3 v^3 + k_1 x + k_3 x^3 + k_5 x^5)q] + \pi K\frac{\partial^2 q}{\partial v^2} \tag{5}$$

where $q = q(x, v, t|x^{(0)}, v^{(0)}, t_0)$. The FPK equation is to be solved under the initial condition [14]

$$q\left(x, v, t_0\middle|x^{(0)}, v^{(0)}, t_0\right) = \delta\left(x - x^{(0)}\right)\delta\left(v - v^{(0)}\right) \tag{6}$$

and some specified boundary conditions.

Generally, the FPK equation is too complicated in its formulation in most cases to be solved exactly in an explicit expression. Therefore, the path integration method is adopted to obtain the PDF solution with the help of the FPK equation. It is worth noticing that the path integration method does not directly solve the FPK equation but it uses the short-time solution to the FPK equation for its short-time transition probability density function during the implementation procedure. The implementation procedure of the path integration method is presented herein as follows.

For the PDF $p(x, v, t)$ at a specified time instant, it can be obtained through the integration from the initial solution $p(x^{(0)}, v^{(0)}, t_0)$

$$p(x, v, t) = \int_\Omega q(x, v, t|x^{(0)}, v^{(0)}, t_0)p(x^{(0)}, v^{(0)}, t_0)\,dx^{(0)}\,dv^{(0)} \tag{7}$$

where Ω is the definition domain of x and v. For a long-time duration from the initial solution, $q(x, v, t|x^{(0)}, v^{(0)}, t_0)$ cannot be solved exactly. Therefore, a feasible way is to divide the long-time duration into a sequence of appropriate short-time intervals as follows:

$$\begin{aligned} p(x, v, t) = &\int_\Omega q(x, v, t|x^{(N-1)}, v^{(N-1)}, t_{N-1}) \\ &dx^{(N-1)}\,dv^{(N-1)} \times \int_\Omega q(x^{(N-1)}, v^{(N-1)}, t_{N-1} \\ &|x^{(N-2)}, v^{(N-2)}, t_{N-2})\,dx^{(N-2)}\,dv^{(N-2)} \\ &\cdots \times \int_\Omega q(x^{(2)}, v^{(2)}, t_2|x^{(1)}, v^{(1)}, t_1) \\ &dx^{(1)}\,dv^{(1)} \times \int_\Omega q(x^{(1)}, v^{(1)}, t_1|x^{(0)}, v^{(0)}, t_0) \\ &p(x^{(0)}, v^{(0)}, t_0)\,dx^{(0)}\,dv^{(0)} \end{aligned} \tag{8}$$

It means that a long-time evolution can be expressed in a sequence of short-time evolutions.

The kernel of the path integration method is how to handle Eq. (8) appropriately. In this paper, the Gauss–Legendre quadrature integration rule is adopted to numerically solve Eq. (8) [15,16]. First the domains of x and v are divided into a number of sub-intervals. Along x-direction, the number of sub-intervals is n. Along v-direction, the number of sub-intervals is m. In each sub-interval, two Gaussian quadrature points are selected by the following way. For the kth interval along x-direction

$$\begin{cases} x_i = x_L + 0.2113(x_R - x_L) \\ x_{i+1} = x_R - 0.2113(x_R - x_L) \end{cases} \tag{9}$$

where $i = (k-1)\times 2 + 1$ and $k = 1, \ldots, n$. x_L is the left boundary of the kth interval and x_R is the right boundary of the kth interval. Similarly, along v-direction,

$$\begin{cases} v_j = v_L + 0.2113(v_R - v_L) \\ v_{j+1} = v_R - 0.2113(v_R - v_L) \end{cases} \tag{10}$$

where $j = (l-1)\times 2 + 1$ and $l = 1, \ldots, m$. v_L is the left boundary of the lth interval and v_R is the right boundary of the lth interval.

For the Gaussian quadrature integration, the corresponding weight equals 1.0 for each integration point. Therefore, instead of Eq. (8), the PDF $p(x_r^I, v_s^I, t_I)$ at the Ith time step is formulated by a summation over the entire domain at the $(I-1)$th time step

$$p(x_r^I, v_s^I, t_I) = \frac{\Delta_x}{2}\frac{\Delta_v}{2}\sum_{i=1}^{2n}\sum_{j=1}^{2m} p\left(x_i^{(I-1)}, v_j^{(I-1)}, t_{I-1}\right)q\left(x_r^{(I)}, v_s^{(I)}, t_I \middle| x_i^{(I-1)}, v_j^{(I-1)}, t_{I-1}\right) \tag{11}$$

where Δ_x and Δ_v are the lengths of sub-intervals along x-direction and v-direction, respectively.

Another crucial problem is about how to formulate the transition probability density function $q(x_r^{(I)}, v_s^{(I)}, t_I|x_i^{(I-1)}, v_j^{(I-1)}, t_{I-1})$ in each short-time step in Eq. (11). Many efforts have been made to establish an adequate transition probability density function. An efficient and accurate way of computing the one-step transition probability density function is the short-time Gaussian approximation given by Sun and Hsu [22]. They discussed that when the interval time was very less than 1.0, the short-time solution to the FPK equation was approximately Gaussian within an error of order of the square of the interval time. The short-time Gaussian transition probability density function can be formulated by the Gaussian closure method. Especially, the jointly Gaussian PDF of two variables (x, v) is given below:

$$\begin{aligned} &q(x_r^{(I)}, v_s^{(I)}, t_I|x_i^{(I-1)}, v_j^{(I-1)}, t_{I-1}) \\ &= \frac{1}{2\pi\sigma_{x_i^{(I-1)}}\sigma_{v_j^{(I-1)}}\sqrt{1-\rho^2_{x_i^{(I-1)}v_j^{(I-1)}}}} \\ &\times \exp\left\{-\frac{1}{2\left(1-\rho^2_{x_i^{(I-1)}v_j^{(I-1)}}\right)}\left[\left(\frac{x_r^{(I)} - m_{x_i^{(I-1)}}}{\sigma_{x_i^{(I-1)}}}\right)^2\right.\right. \\ &- 2\rho_{x_i^{(I-1)}v_j^{(I-1)}}\left(\frac{x_r^{(I)} - m_{x_i^{(I-1)}}}{\sigma_{x_i^{(I-1)}}}\right)\left(\frac{v_s^{(I)} - m_{v_j^{(I-1)}}}{\sigma_{v_j^{(I-1)}}}\right) \\ &\left.\left.+\left(\frac{v_s^{(I)} - m_{v_j^{(I-1)}}}{\sigma_{v_j^{(I-1)}}}\right)^2\right]\right\} \end{aligned} \tag{12}$$

Eq. (11) presents a computational procedure to obtain the PDF evolution step by step, beginning from a specified initial probability density function. Using the Gauss–Legendre quadrature rule, the original continuous PDF solution is approximated by discrete PDF evolution at discrete Gaussian points.

Eq. (12) is a Gaussian PDF which is determined by its conditional means and variances of $x_i^{(I-1)}$ and $v_j^{(I-1)}$. The means and variances can be obtained by the Gaussian closure method. The moment equations associated with Eq. (4) are as follows:

$$\begin{cases} \dot{m}_{10} = m_{01} \\ \dot{m}_{01} = -k_5 m_{50} - k_3 m_{30} - k_1 m_{10} - c_3 m_{03} - c_1 m_{01} \\ \dot{m}_{20} = 2m_{11} \\ \dot{m}_{11} = -k_5 m_{60} - k_3 m_{40} - k_1 m_{20} - c_3 m_{13} - c_1 m_{11} \\ \qquad + m_{02} \\ \dot{m}_{02} = -2k_5 m_{51} - 2k_3 m_{31} - 2k_1 m_{11} - 2c_3 m_{04} \\ \qquad - 2c_1 m_{02} + 2\pi K \end{cases} \tag{13}$$

where $m_{ij} = E[x^i v^j]$. Using the Gaussian closure method, the moments of higher than the second-order can be expressed by the first-order and second-order moments according to the property of a Gaussian probability. These higher-order moments are given below:

$$\begin{cases} m_{30} = 3m_{10}m_{20} - 2m_{10}^3 \\ m_{03} = 3m_{01}m_{02} - 2m_{01}^3 \\ m_{40} = 3m_{20}^2 - 2m_{10}^4 \\ m_{04} = 3m_{02}^2 - 2m_{01}^4 \\ m_{13} = 3m_{02}m_{11} - 2m_{01}^3 m_{10} \\ m_{31} = 3m_{11}m_{20} - 2m_{01}m_{10}^3 \\ m_{50} = 6m_{10}^5 - 20m_{10}^3 m_{20} + 15m_{10}m_{20}^2 \\ m_{60} = 16m_{10}^6 - 30m_{10}^4 m_{20} + 15m_{20}^3 \\ m_{51} = 16m_{01}m_{10}^5 - 10m_{11}m_{10}^4 - 20m_{01}m_{10}^3 m_{20} \\ \qquad + 15m_{11}m_{20}^2 \end{cases} \tag{14}$$

Subsequently, Eqs. (13) and (14) can be solved by the fourth-order Runge–Kutta algorithm. The initial solution at the $(I-1)$th time step for the algorithm is given as

$$\begin{aligned} \mathbf{m}^{(0)} &= \left[m_{10}^{(0)}, m_{01}^{(0)}, m_{20}^{(0)}, m_{11}^{(0)}, m_{02}^{(0)} \right] \\ &= \left[x_i^{(I-1)}, v_j^{(I-1)}, \left(x_i^{(I-1)}\right)^2, x_i^{(I-1)} v_j^{(I-1)}, \left(v_j^{(I-1)}\right)^2 \right] \end{aligned} \tag{15}$$

Because the transition probability density function has a significant value only in the neighborhood of the starting point $(x_i^{(I-1)}, v_j^{(I-1)})$, only a few destination Gauss points are needed in Eq. (11) [16]. The computation at other Gaussian points can be eliminated. For each starting Gaussian point, the selected destination Gauss points are located within the range of $\mu \pm 5\sigma$. For a conventional Gaussian PDF with a mean μ and a standard deviation σ, the range of $\mu \pm 5\sigma$ almost includes the entire portion of a Gaussian distribution. In addition, for a time-invariant system, the time range can be divided into a few uniform time steps. The corresponding transition probability density function equation (12) can be calculated only once and repeatedly used in each time step [15]. These simplifications can significantly reduce the computational cost.

3. Numerical analysis

In this section, three cases are considered for non-linear random ship roll motion. According to Eq. (1), the system parameters are given as follows: $c_1 = 0.1$, $c_3 = 0.1$, $k_1 = 1.0$ and $k_3 = -0.5$. The state space is $[-3, 3] \times [-3, 3]$, which is divided into 40 uniform sub-intervals along each direction with two quadrature points in each sub-interval. Different values of k_5 and $2\pi K$ are taken to examine the effectiveness of the path integration method, which is presented in Table 1. Because exact solutions are unavailable, Monte Carlo simulation is conducted to provide adequate PDF solutions for each case. The sample size is 2×10^4 for transition PDF solutions and 2×10^7 for stationary PDF solutions, respectively. Furthermore, the Gaussian PDF solutions given by the equivalent linearization method are also provided for each case to show the non-Gaussian behavior of non-linear ship roll motion.

Table 1
Parameter settings in the numerical analysis.

Cases	k_5	$2\pi K$	Remarks
Case 1	0.1	0.1	Small fifth-order nonlinearity term
Case 2	1.0	0.1	Large fifth-order nonlinearity term
Case 3	0.1	0.3	High excitation level

The initial PDF is given as

$$p(x^{(0)}, v^{(0)}, 0) = \frac{1}{2\pi\sigma_x\sigma_v} \exp\left\{ -\frac{(x^{(0)} - \mu_x)^2}{2\sigma_x^2} - \frac{(v^{(0)} - \mu_v)^2}{2\sigma_v^2} \right\} \tag{16}$$

where $\mu_x = -2.0$, $\mu_v = -1.8$, $\sigma_x = 0.1$ and $\sigma_v = 0.1$. They are the same as the values given by Yu et al. [15].

3.1. Case 1: Small fifth-order non-linearity term

First a small fifth-order non-linearity term is taken by setting $k_5 = 0.1$ and $2\pi K = 0.1$. The time step is taken as 0.5 for formulating transition PDF solution with short-time Gaussian approximation. The comparison on the transition PDF solution (denoted as TPDF) is presented in Fig. 1 along with the simulation result. In Fig. 1, the transition result obtained with short-time Gaussian approximation is denoted as STGA. The result obtained with Monte Carlo simulation is denoted as MCS. The initial conditions for the transition PDF solution are given with the testing point ($x = 0.2$ and $v = 0.2$). Fig. 1 shows that the transition PDF which is based on short-time Gaussian approximation agrees very well with the simulation result for roll angle and its angular velocity. Therefore, the time step with 0.5 is adequate in the path integration method.

Numerical analysis shows that the computed PDF with the path integration method becomes stationary after $t = 50$ (i.e., 100 steps). Therefore, Fig. 2 presents a comparison on the stationary PDFs obtained with the path integration method (PI), the equivalent linearization method (EQL) and Monte Carlo simulation (MCS). The PDF solution given with the path integration method is at $t = 50$. Fig. 2(a) shows that the PDF solutions coincide with each other very well using each method. However, when the PDF solutions are shown in a logarithmic scale in Fig. 2(b), a significant difference between EQL and MCS can be observed in the low-level probability density. In such a case, the PDF solution obtained with the path integration method is in very good agreement with MCS. Although the fifth-order non-linearity term is small, the third-order non-linearity term is considerably large (i.e., $k_3 = -0.5$). The PDF of roll angle exhibits a significantly non-Gaussian behavior in its tail region.

Another observation is that, compared with the Gaussian PDF (EQL), the PDF of small amplitude roll has a nearly Gaussian distribution near the equilibrium position as shown in Figs. 2(a) and (b). When roll angle gradually increases, the non-linear terms become large in magnitude. The PDF of roll angle becomes softening and later hardening. It is because the sign of the coefficient of the third-order term is negative and it drives the ship motion to exhibit a softening behavior. By contrast, the sign of the coefficient of the fifth-order term is positive leading to a hardening behavior of roll angle. When roll angle is a little far from the equilibrium position, the third-order term is dominant and the PDF of roll angle is softening. When roll angle becomes significantly far from the equilibrium position, the fifth-order term is dominant and the PDF of roll angle becomes hardening. These explain why the actual PDF of roll angle has a various behavior along with the increase of

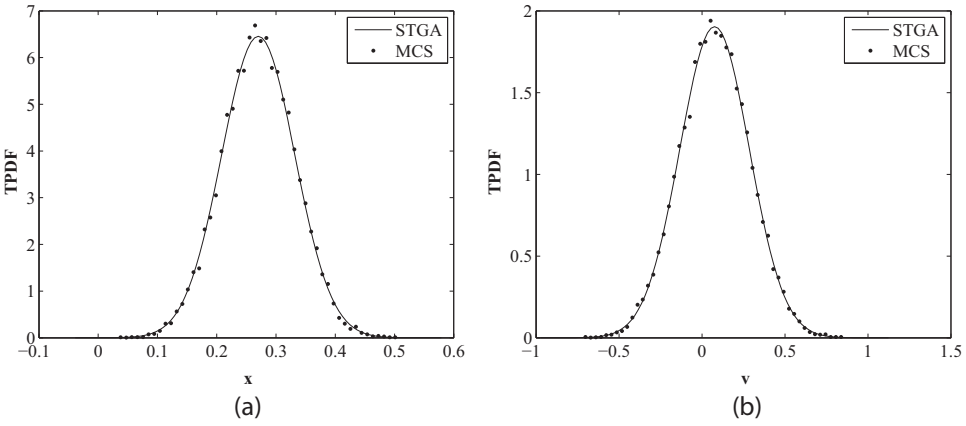

Fig. 1. Comparison of TPDFs in case 1: (a) TPDFs of displacement; (b) TPDFs of velocity.

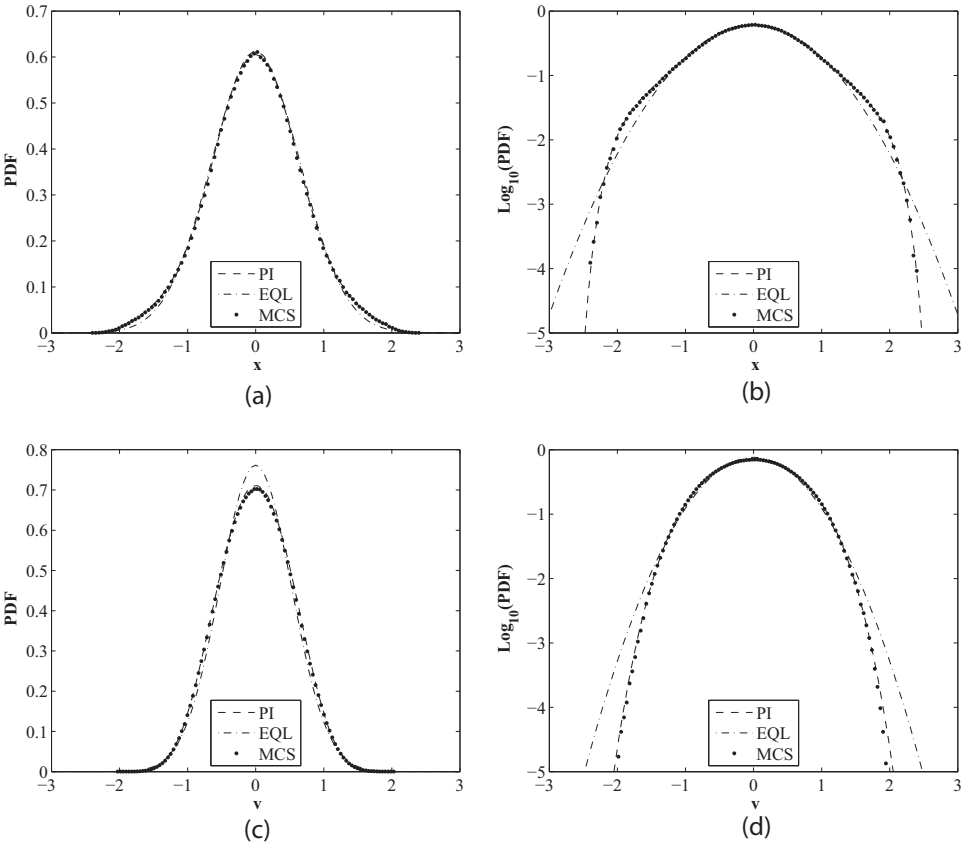

Fig. 2. Comparison of PDFs in case 1: (a) PDFs of displacement; (b) logarithmic PDFs of displacement; (c) PDFs of velocity; (d) logarithmic PDFs of velocity.

roll angle compared with the Gaussian PDF (EQL).

As the angular velocity is concerned in Figs. 2(c) and (d), EQL differs significantly from MCS and the path integration method can provide a satisfactory PDF solution. In the presence of the non-linear third-order damping term, the angular velocity exhibits a hardening behavior in the large response region compared with the Gaussian PDF (EQL). These observations coincide with the conclusions of Chai et al. [40]. The non-linear restoring terms and the non-linear damping terms have a significant influence on the response statistics in the large roll response region. Whereas, the corresponding linear terms mainly have an influence on the response statistics in the low roll response region.

3.2. Case 2: Large fifth-order non-linearity term

Second the coefficient of the fifth-order non-linearity term increases from 0.1 to 1.0 considering the effect of strong non-linearity term. In such a case, it is observed that the time step is taken as 1.0 and the transition PDF solution obtained with short-time Gaussian approximation agrees very well with the simulation result as shown in Fig. 3. The initial conditions for the transition PDF solution are also given with the testing point ($x=0.2$ and $v=0.2$). Fig. 4 presents a comparison on the stationary PDF solutions given by each method. Due to the presence of the large fifth-order non-linearity term, the PDF of the roll angle exhibits a significantly non-Gaussian behavior. The PDF solution given with the path integration method is also at $t=50$. As shown in Figs. 4(a) and (b), MCS is significantly different from EQL. Because EQL denotes a

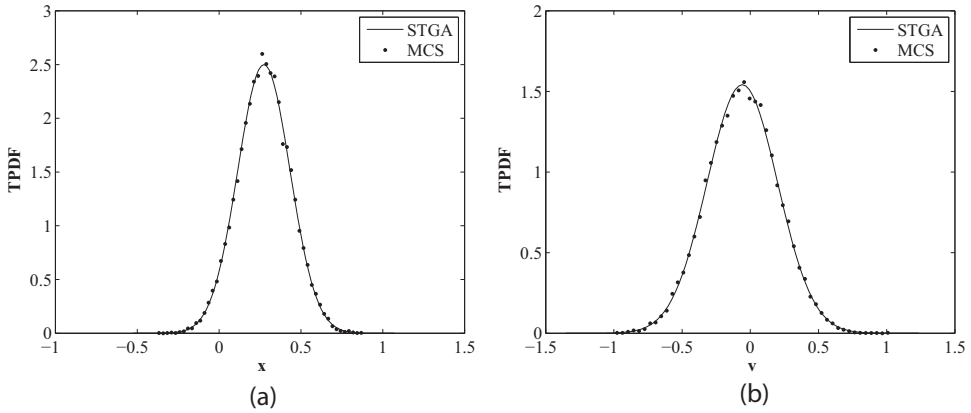

Fig. 3. Comparison of TPDFs in case 2: (a) TPDFs of displacement; (b) TPDFs of velocity.

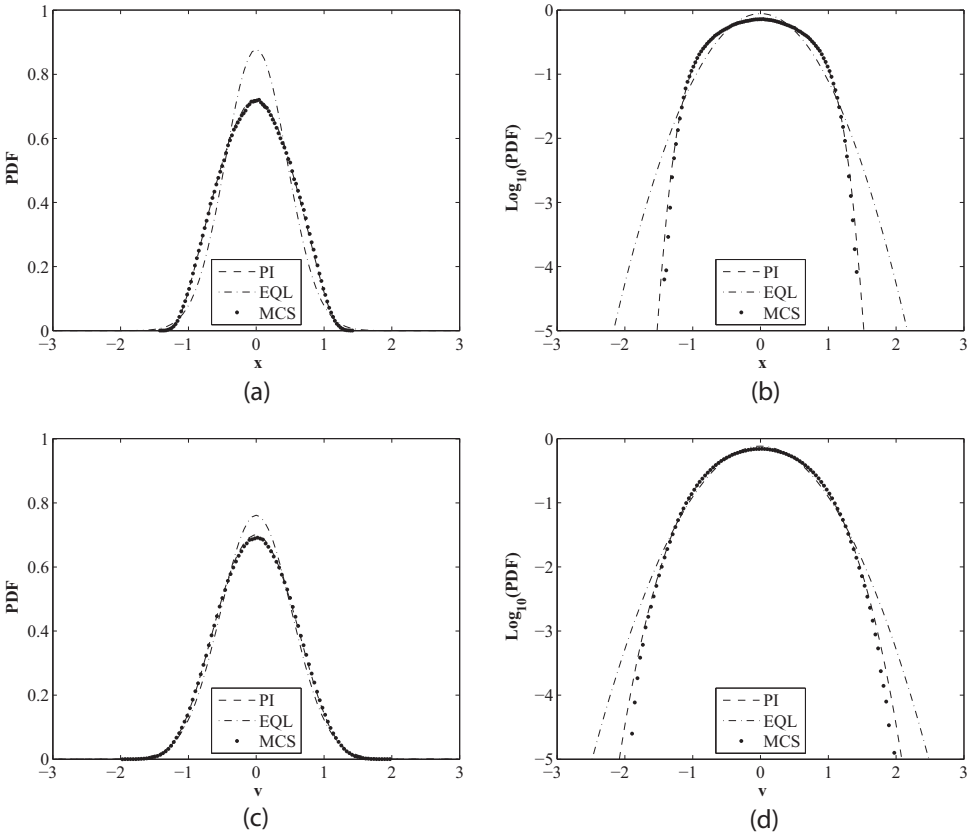

Fig. 4. Comparison of PDFs in case 2: (a) PDFs of displacement; (b) logarithmic PDFs of displacement; (c) PDFs of velocity; (d) logarithmic PDFs of velocity.

Gaussian PDF distribution, the PDF of the roll angle is non-Gaussian. The PDF distribution of roll angle has a similar shape to that of case 1. The PDF of roll angle first becomes softening and then rapidly becomes hardening. Even near the equilibrium position, the PDF of roll angle differs significantly from being Gaussian. This difference from case 1 is due to the large fifth-order non-linearity term. In the small roll response region, the non-linearity term has already a large magnitude. In the case of angular velocity, the similar manner to case 1 is observed as shown in Figs. 4(c) and (d). EQL departs a lot from MCS, and PI is in good agreement with the simulation result. Due to the presence of the non-linear third-order damping term, the angular velocity exhibits a hardening behavior compared with the Gaussian PDF (EQL).

3.3. Case 3: High excitation level

At last, the coefficient of the small fifth-order non-linearity term is kept as 0.1. The excitation intensity increases from 0.1 to 0.3. This section considers the effect of excitation intensity. In this case, the time step is taken as 0.5 and the transition PDF solution obtained with short-time Gaussian approximation agrees very well with the simulation result as shown in Fig. 5. Similarly, the initial conditions for the transition PDF solution are given with the testing point ($x=0.2$ and $v=0.2$).

Fig. 6 presents a comparison on the stationary PDF solutions given by each method. The PDF solution given with the path integration method is at $t=50$. Due to the increase of excitation intensity, the PDF of the roll angle also exhibits a significantly non-Gaussian behavior although the coefficient of the fifth-order non-linearity term is small. It is because the strong excitation intensity

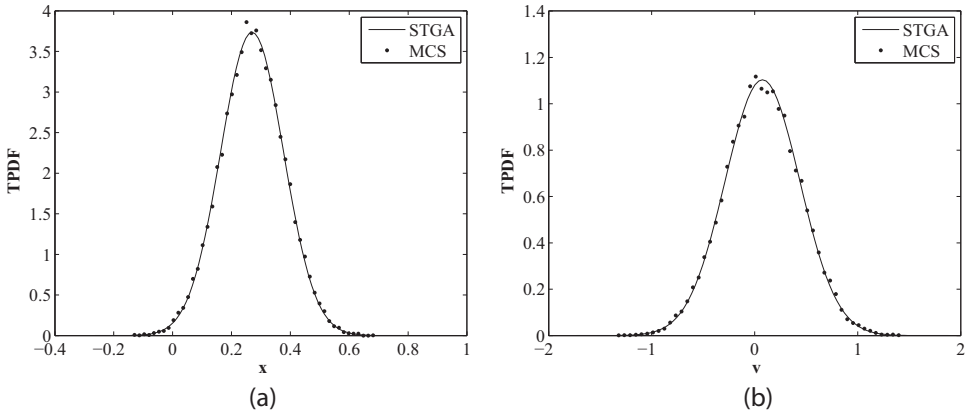

Fig. 5. Comparison of TPDFs in case 3: (a) TPDFs of displacement; (b) TPDFs of velocity.

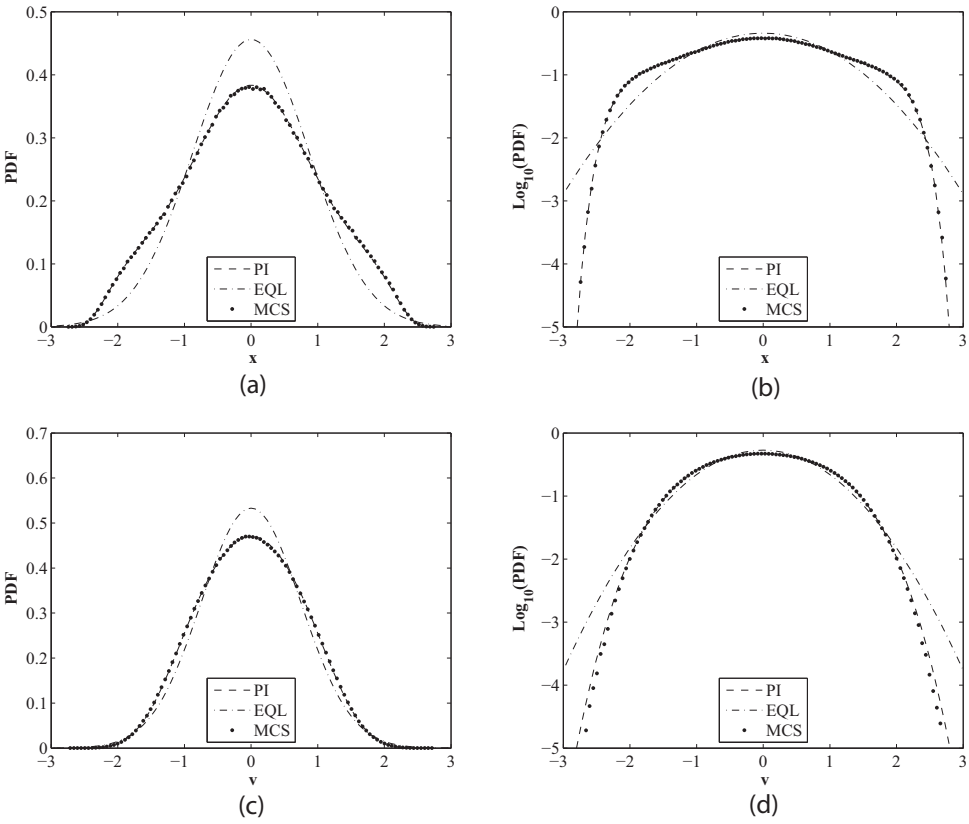

Fig. 6. Comparison of PDFs in case 3: (a) PDFs of displacement; (b) logarithmic PDFs of displacement; (c) PDFs of velocity; (d) logarithmic PDFs of velocity.

leads to large magnitudes of roll angle. This also results in large non-linearity terms. As shown in Figs. 6(a) and (b), MCS differs significantly from EQL showing that the PDF of roll angle is non-Gaussian. In the case of angular velocity, the similar manner to case 1 is observed as shown in Figs. 6(c) and (d). EQL differs a lot from MCS, and PI agrees well with the simulation result. Due to the presence of the non-linear third-order damping term, the angular velocity exhibits a hardening behavior compared with the Gaussian PDF (EQL).

Due to the increase of the excitation intensity, the subsequent roll angle and angular velocity increase. Therefore, their PDF distributions have wider ranges than those of cases 1 and 2. Correspondingly, the peaks of their PDF distributions in the central region are lower than those of cases 1 and 2. These also coincide with the observations of Chai et al. [40].

4. Conclusions

A path integration analysis is conducted on non-linear random ship roll motion. The mathematical model of ship rolling motion is adopted using a linear-plus-cubic damping and a non-linear restoring moment in the form of odd-order polynomials up to fifth-order terms. In the solution procedure, the interpolation scheme is based on the Gauss–Legendre quadrature integration rule and the short-time transition probability density function is based on short-time Gaussian approximation. The present study applies the path integration method to the case of non-linear random ship roll motion. In order to show the effectiveness of the path integration method, different values of non-linearity coefficient and excitation intensity are considered. Numerical analysis shows that the path integration solutions agree well with the results given by Monte Carlo simulation, even in the tail region of probability density. The

path integration method is effective and simply implemented in the examined cases. Numerical analysis further shows that in the large roll response region, the non-linear restoring terms and the non-linear damping terms have a significant influence on the response statistics. The corresponding linear terms mainly have an influence on the response statistics in the low roll response region. Even in the case of small non-linearity terms, the increase of the excitation intensity also leads to a highly non-Gaussian behavior of non-linear ship roll motion.

Acknowledgments

This research is jointly supported by the National Natural Science Foundation of China under Grant no. 51478311, the Natural Science Foundation of Tianjin, China under Grant no. 14JCQNJC07400 and the Innovation Foundation of Tianjin University under Grant no. 60301014.

References

[1] T.K. Caughey, F. Ma, The exact steady-state solution of a class of non-linear stochastic systems, Int. J. Non-Linear Mech. 17 (1982) 137–142.
[2] M.F. Dimentberg, An exact solution to a certain non-linear random vibration problem, Int. J. Non-Linear Mech. 17 (1982) 231–236.
[3] W.Q. Zhu, Z.L. Huang, Exact stationary solutions of stochastically excited and dissipated partially integrable Hamiltonian systems, Int. J. Non-Linear Mech. 36 (2001) 39–48.
[4] T.K. Caughey, Equivalent linearization techniques, J. Acoust. Soc. Am. 35 (1963) 1706–1711.
[5] P.D. Spanos, Stochastic linearization in structural dynamics, Appl. Mech. Rev. 34 (1981) 1–8.
[6] J.B. Roberts, P.D. Spanos, Random Vibration and Statistical Linearization, Dover Publications Inc., Mineola, New York, 2003.
[7] J.B. Roberts, P.D. Spanos, Stochastic averaging: an approximate method of solving random vibration problems, Int. J. Non-Linear Mech. 21 (1986) 111–134.
[8] J.Q. Sun, C.S. Hsu, Cumulant-neglect closure method for nonlinear systems under random excitations, J. Appl. Mech. 54 (1987) 649–655.
[9] R.S. Langley, A finite element method for the statistics of non-linear random vibration, J. Sound Vib. 101 (1985) 41–54.
[10] B.F. Spencer Jr., L.A. Bergman, On the numerical solution of the Fokker–Planck equation for nonlinear stochastic systems, Nonlinear Dyn. 4 (1993) 357–372.
[11] S.F. Wojtkiewicz, E.A. Johnson, L.A. Bergman, M. Grigoriu, B.F. Spencer Jr., Response of stochastic dynamical systems driven by additive Gaussian and Poisson white noise: solution of a forward generalized Kolmogorov equation by a spectral finite difference method, Comput. Methods Appl. Mech. Eng. 168 (1999) 73–89.
[12] M. Shinozuka, Monte Carlo solution of structural dynamics, Comput. Struct. 2 (1972) 855–874.
[13] M.F. Wehner, W.G. Wolfer, Numerical evaluation of path-integral solutions to Fokker–Plank equations, Phys. Rev. A 27 (1983) 2663–2670.
[14] A. Naess, J.M. Johnsen, Response statistics of nonlinear, compliant offshore structures by the path integral solution method, Probab. Eng. Mech. 8 (1993) 91–106.
[15] J.S. Yu, G.Q. Cai, Y.K. Lin, A new path integration procedure based on Gauss–Legendre scheme, Int. J. Non-Linear Mech. 32 (1997) 759–768.
[16] J.S. Yu, Numerical path integration of stochastic systems (Ph.D. thesis), Florida Atlantic University, 1997.
[17] M.F. Wehner, W.G. Wolfer, Numerical evaluation of path-integral solutions to Fokker–Planck equations. II. Restricted stochastic processes, Phys. Rev. A 28 (1983) 3003–3011.
[18] M.F. Wehner, W.G. Wolfer, Numerical evaluation of path-integral solutions to Fokker–Planck equations. III. Time and functionally dependent coefficients, Phys. Rev. A 35 (1987) 1795–1801.
[19] C.S. Hsu, H.M. Chiu, A cell mapping method for nonlinear deterministic and stochastic systems—part I: the method of analysis, J. Appl. Mech. 53 (1986) 695–701.
[20] H.M. Chiu, C.S. Hsu, A cell mapping method for nonlinear deterministic and stochastic systems—part II: examples of application, J. Appl. Mech. 53 (1986) 702–710.
[21] J.Q. Sun, C.S. Hsu, First-passage time probability of non-linear stochastic systems by generalized cell mapping method, J. Sound Vib. 124 (1988) 233–248.
[22] J.Q. Sun, C.S. Hsu, The generalized cell mapping method in nonlinear random vibration based upon short-time Gaussian approximation, J. Appl. Mech. 57 (1990) 1018–1025.
[23] S.H. Crandall, K.L. Chandiramani, R.G. Cook, Some first-passage problems in random vibration, J. Appl. Mech. 33 (1966) 532–538.
[24] S.H. Crandall, First-crossing probabilities of the linear oscillator, J. Sound Vib. 12 (1970) 285–299.
[25] A. Naess, V. Moe, Efficient path integration methods for nonlinear dynamic systems, Probab. Eng. Mech. 15 (2000) 221–231.
[26] Y. Wang, A path integration algorithm for stochastic structural dynamic systems, Appl. Math. Comput. 228 (2014) 423–431.
[27] A. Pirrotta, R. Santoro, Probabilistic response of nonlinear systems under combined normal and Poisson white noise via path integral method, Probab. Eng. Mech. 26 (2011) 26–32.
[28] G. Cottone, M. Di Paola, R. Ibrahim, A. Pirrotta, R. Santoro, Stochastic ship roll motion via path integral method, Int. J. Nav. Arch. Ocean 2 (2010) 119–126.
[29] I.A. Kougioumtzoglou, P.D. Spanos, An analytical Wiener path integral technique for non-stationary response determination of nonlinear oscillators, Probab. Eng. Mech. 28 (2012) 125–131.
[30] I.A. Kougioumtzoglou, P.D. Spanos, Stochastic response analysis of the softening Duffing oscillator and ship capsizing probability determination via a numerical path integral approach, Probab. Eng. Mech. 35 (2014) 67–74.
[31] M.F. Dimentberg, O. Gaidai, A. Naess, Random vibrations with strongly inelastic impacts: response PDF by the path integration method, Int. J. Non-Linear Mech. 44 (2009) 791–796.
[32] L. Liu, Y. Tang, The random jumping of ship rolling in narrowband wave considering the static effect of liquid on board, J. Vib. Control 19 (2013) 576–584.
[33] H.U. Köylüoglu, S.R.K. Nielsen, R. Iwankiewicz, Response and reliability of Poisson-driven systems by path integration, J. Eng. Mech. 121 (1995) 117–130.
[34] H.U. Köylüoglu, S.R.K. Nielsen, A.Ş. Çakmak, Fast cell-to-cell mapping (path integration) for nonlinear white noise and Poisson driven systems, Struct. Saf. 17 (1995) 151–165.
[35] M. Di Paola, R. Santoro, Non-linear systems under Poisson white noise handled by path integral solution, J. Vib. Control 14 (2008) 35–49.
[36] M. Di Paola, R. Santoro, Path integral solution for non-linear system enforced by Poisson white noise, Probab. Eng. Mech. 23 (2008) 164–169.
[37] Y.G. Wang, J.H. Tan, Path integral solution of a strongly nonlinear stochastic oscillation system, J. Vib. Shock 26 (2007) 153–155 (in Chinese).
[38] Y.G. Wang, J.H. Tan, Markov modeling for slow drift oscillations of moored vessels in irregular waves, J. Ship Mech. 12 (2008) 368–376.
[39] Y.G. Wang, J.H. Tan, L.P. Xue, On the exceedance probabilities of extreme drift motions of an offshore structure, China Ocean Eng. 23 (2009) 27–35.
[40] W. Chai, A. Naess, B.J. Leira, Stochastic dynamic analysis and reliability of a vessel rolling in random beam seas, J. Ship Res. 59 (2015) 113–131.
[41] N.G. Van Kampen, A cumulant expansion for stochastic linear differential equations. I, Physica 74 (1974) 215–238.
[42] N.G. Van Kampen, A cumulant expansion for stochastic linear differential equations. II, Physica 74 (1974) 239–247.
[43] E. Meeron, Series expansion of distribution functions in multicomponent fluid systems, J. Chem. Phys. 27 (1957) 1238–1246.